Measuring interpersonal transmission of expiratory droplet nuclei in close proximity

Fu, Linzhi; Nielsen, Peter V.; Wang, Yi; Liu, Li

Published in:
Indoor and Built Environment

DOI (link to publication from Publisher):
10.1177/1420326X211029689

Publication date:
2022

Document Version
Accepted author manuscript, peer reviewed version

Page Proof Instructions and Queries

Journal Title: Indoor and Built Environment (IBE)

Article Number: 1029689

Thank you for choosing to publish with us. This is your final opportunity to ensure your article will be accurate at publication. Please review your proof carefully and respond to the queries using the circled tools in the image below, which are available in Adobe Reader DC* by clicking **Tools** from the top menu, then clicking **Comment.**

Please use *only* the tools circled in the image, as edits via other tools/methods can be lost during file conversion. For comments, questions, or formatting requests, please use T. Please do *not* use comment bubbles/sticky notes.

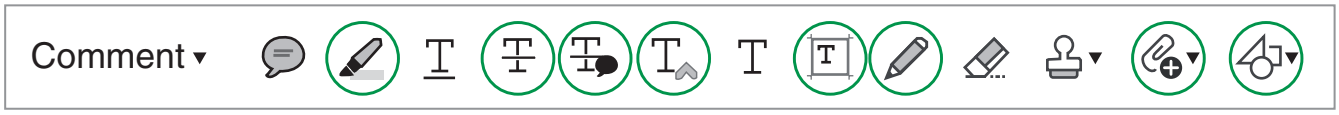

*If you do not see these tools, please ensure you have opened this file with Adobe Reader DC, available for free at get.adobe.com/reader or by going to Help > Check for Updates within other versions of Reader. For more detailed instructions, please see us.sagepub.com/ReaderXProofs.

No.	Query
	Please note that we cannot add/amend ORCID iDs for any article at the proof stage. Following ORCID's guidelines, the publisher can include only ORCID iDs that the authors have specifically validated for each manuscript prior to official acceptance for publication.
	Please confirm that all author information, including names, affiliations, sequence, and contact details, is correct.
	Please review the entire document for typographical errors, mathematical errors, and any other necessary corrections; check headings, tables, and figures.
	Please confirm that the Funding and Conflict of Interest statements are accurate.
	Please ensure that you have obtained and enclosed all necessary permissions for the reproduction of artistic works, (e.g. illustrations, photographs, charts, maps, other visual material, etc.) not owned by yourself. Please refer to your publishing agreement for further information.
	Please note that this proof represents your final opportunity to review your article prior to publication, so please do send all of your changes now.
AQ: 1	Please check the sentence 'When ordered by *IF*,. . .' for clarity.
AQ: 2	Please mention the accessed date for the URL in ref. 20.
AQ: 3	Please mention the accessed date for the URL in ref. 38.
AQ: 4	Please mention the accessed date for the URL in ref. 41.
AQ: 5	Please provide the in-text citation for Table 2.
AQ: 6	Please check and confirm all figure captions are correct.

Special Issue: Prevention and control of COVID-19 transmission in the indoor environment

Indoor and Built Environment

Indoor and Built Environment
0(0) 1–13

DOI: 10.1177/1420326X211029689
journals.sagepub.com/home/ibe

SAGE

Measuring interpersonal transmission of expiratory droplet nuclei in close proximity

Linzhi Fu[1,2], Peter V. Nielsen[3], Yi Wang[1,4] and Li Liu[5,6]

Abstract

Increasing evidence supports the significant role of short-range airborne transmission of viruses when in close contact with a source patient. A full-scale ventilated room (Cleanliness: ISO 14644–1 Class 5) and two face-to-face standing breathing thermal manikins were used to simulate a source individual and a susceptible person. Monodisperse particle generation and measurement techniques were used to evaluate the effect of virus-laden droplet nuclei size on short-range airborne transmission risk. We analysed four particle sizes (1.0, 1.5, 2.5, and 5 μm) to simulate the transport of exhaled droplet nuclei within an interpersonal distance of 0.5 m. The results indicated that the size distribution of airborne droplet nuclei could significantly influence transmission, with the inhalation fraction decreasing with increasing droplet nuclei size. Additionally, results showed that proximity to the source manikin could influence transmission. Inhalation fraction decreased with increasing interpersonal distance, fitting well with the $1/d$ rule of droplet nuclei concentration decay. Our findings improve the understanding of the mechanism of the disease transmission.

Keywords

Inhalation fraction, Airborne, Short-range, COVID-19

Accepted: 14 June 2021

Introduction

As of 21 April 2021, there have been 142,238,078 confirmed cases of severe acute respiratory syndrome coronavirus 2 (SARS-CoV-2) and 3,032,124 confirmed deaths across 223 countries, areas, or territories. There are three common transmission routes for respiratory pathogens (such as SARS-CoV-2): droplet, contact and aerosol (or airborne) transmission. Throughout the coronavirus disease 2019 (COVID-19) pandemic, there has been much debate over the transmission of SARS-CoV-2.[1,2] Airborne transmission is the primary transmission route of SARS-CoV-2, via inhalation of droplets/nuclei exhaled by an infected individual. Several lines of evidence support the hypothesis that SARS-CoV-2 transmission is predominantly airborne.[3,4] Therefore, we must adapt our indoor environment control strategies to address the potential implications of airborne SARS-CoV-2 transmission.[5,6]

SARS-CoV-2 most commonly spreads between people during periods of close contact.[7,8] Indoor environments, such as homes and workplaces, are the most common sites of SARS-CoV-2 transmission,[9] with the highest risk of transmission seen in households.[10] Research has confirmed that shared indoor

[1]State Key Laboratory of Green Building in Western China, Xi'an University of Architecture and Technology, Xi'an, China
[2]School of Resources Engineering, Xi'an University of Architecture and Technology, Xi'an, China
[3]Department of Civil Engineering, Aalborg University, Aalborg, Denmark
[4]School of Building Services Science and Engineering, Xi'an University of Architecture and Technology, Xi'an, China
[5]Department of Building Science, School of Architecture, Tsinghua University, Beijing, China
[6]Laboratory of Eco-Planning & Green Building, Ministry of Education, Tsinghua University, Beijing, China

Corresponding author:
Li Liu, Department of Building Science, School of Architecture, Tsinghua University, Beijing 100084, China.
Email: liuli_archi@tsinghua.edu.cn

space is a major risk factor for viral transmission.[11] Close contact is known to play an important role in the spread of many respiratory diseases.[12] People may become infected easily when in proximity to individuals suffering from COVID-19.[13] Close contact transmission includes short-range airborne, large-droplet and direct contact transmission.[14] Short-range airborne transmission via exhaled droplets/nuclei predominates when in close contact with a source patient.[15] Short-range airborne transmission appears to mechanistically dominate close-range transmission of SARS-CoV-2, which is why social distancing works so effectively to combat the spread of COVID-19. Inhalation of microscopic respiratory droplets containing viruses is possible at short-range to long-range distances.[16] The higher the concentration of infectious particles, and thus greater the risk of infection, at a short-range from an infectious source (<1 m) is significantly higher than that at a long range (>2 m).[1] However, despite this, short-range airborne transmission routes have largely been overlooked.[17]

Infectious pathogens filled with lung fluid spread via respiratory droplets. The key processes in the transmission routes of respiratory pathogens are affected by the generation, transportation and inhalation of these respiratory droplets. The number contribution and size distribution of the particles that are generated by different respiratory activities, such as normal breathing from the nose or mouth, coughing, sneezing, singing and talking, are different. Pathogens found on the surface of an infected person's respiratory airways can become encapsulated within a particle that is exhaled during breathing (or coughing).[18,19]

There are currently different opinions on the transmission route of SARS-CoV-2.[19] COVID-19 does not appear to be spread by typical means, especially in the case of superspreading events. Individuals infected with SARS-CoV-2 produce both droplets and aerosols frequently; however, the majority of these emissions do not infect others.[19] Successful airborne transmission requires the exposure of susceptible individuals to droplet/nuclei containing infectious virions at doses sufficient to initiate infection within their respiratory system.[20]

The generation, transport and final destination (inhalation or deposition) of infectious droplets/nuclei are thus key processes in viral transmission.[21,22] Droplet size is a crucial variable that influences inhalation risk and thus disease transmission. Moreover, traditional transmission modes (direct, indirect, large droplet or airborne/aerosol) are affected by carrier droplet/nuclei size.

Individuals typically generate droplets or droplet nuclei with a broad size distribution. The size distribution is often multimodal, reflecting the origin of droplets in different regions of the respiratory airway. Studies on cough aerosols and exhaled breath from patients suffering from various respiratory tract infections have shown that particle size distribution is surprisingly similar between such patients, i.e. smaller particles (<5 μm) predominate.[23] Fine-particle exhaled aerosols occur in lung infections, with the lower airway tract contributing more to the viral aerosols than the upper airway.[24] Most particles in exhaled breath have a diameter smaller than 4 μm, with a median of 0.7–1.0 μm.[25] Aerosolized particles of SARS-CoV-2 have been reported to fall into two broad categories, viz., sub-micrometer particles (0.25–1.0 μm) and supermicrometer particles (>2.5 μm), and can remain suspended in the air for more than 2 h.[26] Similarly, another study reported SARS-CoV-2-containing particles ranging from 1 to 4 μm in size.[27] The virion remained viable in these airborne particles for more than an hour.[28,29] Several studies have focused on the size distribution of droplets/nuclei exhaled by healthy and infected subjects by various means, including breathing, talking and coughing, as summarized in Table 1. Studies examining particles produced by coughing and exhalation have consistently identified pathogens in small particles (<4.7 μm),[23] and one study reported that the minimum diameter of an exhaled particle capable of containing SARS-CoV-2 is approximately less than 4.7 μm.[30]

There is a strong evidence suggesting that many SARS-CoV-2-infected individuals are either minimally symptomatic or asymptomatic.[37] Asymptomatic patients do not experience symptoms such as sneezing and coughing. As such, violent flow events occur less and large droplets are not frequently generated.[11] Despite this, asymptomatic patients have been found to remain highly contagious.[43] In the case of the influenza virus, one study reported that sneezing and coughing are not required for aerosolization.[24] Research showed that normal breathing can emit more viable aerosolized viruses over time than coughing, as the latter is a less frequent activity.[44] Thus, airborne transmission likely occurs during regular daily actions, such as breathing and talking.

Most studies have used smoke and tracer gas,[45–49] rather than actual droplets/nuclei or computational fluid dynamics (CFD) simulations,[17,48,49] to study the distribution, transmission and cause of inhalation-mediated infection. Droplet size distribution is the most important factor affecting diffusion and sedimentation. Therefore, analysing the mechanism of disease transmission via droplet and short-range airborne transmission is very important. Although our understanding of the mechanism of interpersonal cross-infection continues to deepen, thus far, engineering controls that can completely prevent infection have

Table 1. Information from articles on droplet/nuclei size distribution and number distribution of respiratory activity.

	Results				
References	Breath		Cough	Talk	Sing
Duguid[31]	Mouth: >20 μm 15 pt/min		8200 droplets	10–1000 μm 63 droplets	
Loudon and Roberts[32]			81 μm 41,857 droplets		4014 droplets
Papineni and Rosenthal[33]	Mouth	<1 μm 12.5 pt/dm^3 >1 μm 1.9 pt/dm^3	<1 μm 83.2 pt/dm^3 >1 μm 13.4 pt/ dm^3	<1 μm 19.2 pt/dm^3 >1 μm 3.3 pt/dm^3	
	Nose	<1 μm 4.7 pt/dm^3 >1 μm 0.7 pt/dm^3			
Chao et al.[34]		13.5 μm (947–2085 pt/cough)			
Morawska et al.[35]		98 pt/dm^3	678 pt/dm^3	Whispering 'aah' 672 pt/dm^3 voiced 'aah' 1088 pt/dm^3 whispering counting 100 pt/dm^3 voiced counting 130 pt/dm^3	
Asadi et al.[36]					1–50 pt/s
Alsved et al.[29]		135 pt/s		270 pt/s	690 pt/s
Asadi et al.[37]		0.28 pt/s		10.1 pt/s	2.74 pt/s
Hartmann et al.[38]	Nose Mouth	23 pt/s 134 pt/s	13,709 pt/cough		195 pt/s
Li et al.[39]			42.9 (0.3 m), 19.8(0.9m), 3.8 (1.2 m) pt/cm^3		
Mürbe et al.[40]				16–267 pt/s	141–1240 pt/s
Hamilton et al.[41]	Healthy: 0.039 pt/ cm^3 Patient: 0.288 pt/ cm^3		Healthy: 1.400 pt/ cm^3 Patient: 9.79 pt/ cm^3	Healthy: 0.113 pt/ cm^3 Patient: 0.332 pt/ cm^3	
Gregson et al.[42]	Nose–mouth 0.23 pt/cm^3 Nose–nose 0.16 pt/cm^3		1.8 pt/cm^3	0.11 pt/cm^3	0.53 pt/cm^3

pt: Particle.

not been developed. Therefore, effective control strategies are fundamental to the knowledge of the transmission of respiratory pathogens.

The inhalation of exhaled droplet nuclei by a susceptible person in the indoor environment is affected by a complex interaction of various airflows, including respiratory flow, thermal plume and ventilation.[50–54] Early experiments considered with the influence of type of ventilation system, distance, breathing pattern through nose and mouth.[52] The influence of the human exhalation on flow fields, contaminant distributions and personal exposure in displacement ventilated rooms together with effects of physical movement is the first reported literature based on aerosols dynamics (both measurements and CFD).[55] Interpersonal distance (e.g. $\leq$1.5–2 m) determines the dominant air flow. For short-range interactions, the human environment, including respiratory flow and thermal plume, plays a key role in determining the inhalation risk.

In this study, we focus on disease transmission by droplet nuclei, which may remain airborne for hours. We aimed to explore the dynamics of exhaled droplet nuclei between face-to-face standing sources and susceptible individuals, and how they are affected by particle size distribution. The whole process was governed by the complex interaction of respiratory airflow, human thermal plume and ventilation airflow. The interaction of three flows increased the flow turbulence in the breathing zone of the susceptible manikin and the dynamic of interpersonal exposure. Displacement ventilation introduces a low-momentum stream of cold and clean air at the floor level to displace the contaminated air. Displacement ventilation produced a stable stratification. It does not destroy the dynamic process of the interaction of respiratory airflow, human thermal plume and ventilation airflow. The dynamic measurement of the susceptible person's instantaneous inhalation exposure would be beneficial to these studies.

Experiments were conducted in a clean test room with a displacement ventilation system. Particle generation and monitoring coupled with breathing thermal manikins (BTMs) enabled us to examine short-range airborne transmission of the particles. The influence

of the human environment and ventilation flow were key considerations. The results indicated an important role for droplet nuclei size in the short-range airborne transmission of respiratory viruses. An inhalation fraction (*IF*) was defined to quantify exposure risk, while inhalation transmission was reflected in the number of particles inhaled over a period. We, therefore, suggest the adoption of improved respiratory infection control strategies, building upon the traditional understanding of airborne transmission of viruses.

Methods and design

Full-scale room and instruments

The experiments were carried out in a full-scale ventilated room of 5.0 m (length) × 3.5 m (width) × 2.5 m (height) at the State Key Laboratory of Green Building Materials, Xi'an University of Architecture and Technology. The room was a Class 5 cleanroom according to the ISO 14644–1:2015 standard, with displacement/mixing ventilation occurring at a rate of 0.5–20 air changes per hour. Air supply and exhaust outlets measured 0.48 m × 0.48 m each, with each side equipped with a high-efficiency particulate air filter (filtration efficiency > 99.95%). Displacement ventilation experiments (Archimedes number = 45.01×10^3) were used to ensure an air supply temperature of 18 ± 0.5 °C using intelligent control. Supply flow was maintained at 100.5 m^3/h with an air change rate of 2.3 times/h with displacement ventilation. The airflow velocity in the occupied zone was < 0.2 m/s, fulfilling thermal comfort requirements.

The breathing thermal manikins were equally divided into source manikin and susceptible manikin groups, as shown in Figure 1. Manikins were designed according to the average size of an European female, with a height of 1.70 m and a body surface area (BSA) of 1.44 m^2. To accurately simulate human thermal plume, reflecting the impact of body geometry and the diffusion of indoor air pollutants, life-size manikins were used. The inner cavity was surrounded by an aluminium casing with an evenly distributed heating wire connected to a power regulator, allowing body temperature regulation. The manikin's mouth was a semi-elliptical opening with an area of approximately 120 mm^2 along the horizontal direction, and the nostrils consisted of two cylindrical copper tubes with a diameter of 12 mm. The two manikins were internally heated for 12 h with a power of 78.4 W. Under most conditions, face-to-face orientation leads to the highest risk of infection. Thus, the manikins were placed face-to-face in a standing position with a nasal spacing of 0.5 m.

Given that the air exhaled by an infected individual can easily circulate into the breathing area of a nearby individual, the air exhaled by the susceptible individual can exert a net 'cleaning' effect on the breathing area by displacing infected air. Thus, a vibrating orifice aerosol generator (VOAG) 3450 was used to generate monodisperse NaCl particles at a flow rate of 10 dm^3/min to simulate droplets exhaled by the source individual, similar to the initial droplet size distribution of a real person's exhalation. Thus, vibrating orifice aerosol generator VOAG 3450 that generates 1.0 µm, 1.5 µm, 2.5 µm, 5.0 µm monodisperse NaCl particles with a clean air flow rate of 10 dm^3/ min was used to simulate source manikin produce exhale droplets/nuclei. The source manikin exhaled air was heated at 32 ± 1 °C. This study used an artificial lung to simulate a female's periodic breathing cycle. Normal breathing flow was set to 8.36 dm^3/min, corresponding to an expiratory

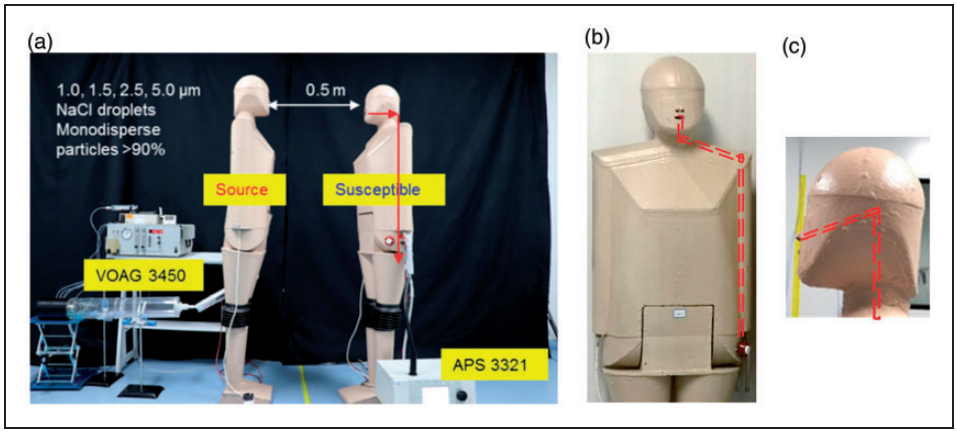

Figure 1. (a) Layout of experiment instruments; (b) Arrangement of the breathing tube with nose inhalation inside the manikin; (c) Breathing tube inside manikin's head. Breathing thermal manikins were positioned standing face-to-face in a full-scale clean room with displacement ventilation. [AQ6]

flow velocity of 2.14 m/s measured by draught probe, with a frequency of 15 breaths/min. The source manikin's exhaled air was heated to 32 ± 1 °C. An aerodynamic particle size spectrometer (APS 3321, particle size range: 0.5–20 μm) with a sample airflow rate of 5 dm^3/min was connected to the susceptible manikin's nose, and the sampling interval was 1 s. The air flow rates through the source and susceptible manikins were detected using a TSI 4143 type mass flow meter. The equipment layout and instrument are shown in Figure 1 and Table 3.

Monodispersed particles of 1.0, 1.5, 2.5 and 5.0 μm in diameter were produced by the VOAG 3450. The instrument generated 43 μm NaCl droplets, and the solvent was evaporated by dilution air. The flow rate was 8.3 cm^3/h, and the dilution air flow rate was 10 dm^3/min. The susceptible individual was exposed to the particle suspensions for 1 h. The experiments were repeated five times ($n = 5$).

Experimental procedures

The measurement process was divided into four steps, whereby the following concentrations were determined:

1. Background level of particles in the room.
2. Monodispersed particles at the mouth of the source manikin when stably released by the VOAG 3450 at the start of the experiment.
3. Monodispersed particles in the inhalation tube of the susceptible manikin.
4. Monodispersed particles at the mouth of the source manikin at the end of the experiment.

Table 2. Parameters for the two thermal breathing manikins. [AQ5]

Parameters	Source manikin	Susceptible manikin
Heating (W)	78.4	78.4
Breathing pattern	Out mouth	In nose
Breathing frequency (min^{-1})	–	15
Respiratory flow (dm^3/min)	10	8.36

Source manikin emission rate and monodisperse particle size distribution

The source manikin emitted monodispersed particles of 1.0, 1.5, 2.5 and 5.0 μm diameter with geometric standard deviations of 1.12, 1.10, 1.05 and 1.09 μm, respectively. The number of particles released at the start and end of the experiment differed by less than 7%, indicating that NaCl particle production remained stable during the experiments (as shown in Figure 2 red box chart and y axis on the left). The mean source manikin emission rates were 35, 68, 152 and 83 pt/s for 1.0 μm, 1.5 μm, 2.5 μm and 5.0 μm, respectively.

An aerodynamic particle size spectrometer (APS 3321) was used to determine the ambient particle concentration prior to commencing the experiment. Background particle concentration was 2.45 ± 0.26 pt/dm^3, which was lower than the exhaled NaCl particle concentration. The background concentration was excluded from two aspects:

First, there were no other sources of particles except particles of a certain size distribution that were released by our experiment. This is because a full-scale room was a Class 5 cleanroom according to the ISO 14644–1:2015 standard. Air supply and exhaust outlets were equipped with a high-efficiency particulate air filter (filtration efficiency > 99.95%) to maintain the cleanliness. During the experiment, personnel wear clean clothes, goggles and masks, and enter the environmental chamber after being air showered to minimize the generation of particles by persons. Second, the room background concentration and the concentration of breathing tube inside the manikin were measured before starting each experiment. The two concentrations were stable and far less than the exhaled monodisperse NaCl particle concentration. In this way, the

Table 3. List of instruments and specifications.

Instrument	Mode	Range	Error
Vibrating orifice aerosol generator	TSI 3450	Generates particles from 1 to 200 μm	GSD <1.2
Aerodynamic Particle sizer	TSI 3321	0.5–20 μm aerodynamic size, 32 channels, 1000 pt/cm^3	10%
Mass flowmeters	TSI 4143	0.01–20 dm^3/min	±2% of reading
Data acquisition	KEYSIGHT 34970A	–	–
Thermocouples	Type K	Temperature range: 0–50°C	±0.1 °C
ComfortSense Main frame	Dantec 54N90	–	–
Draught probe	Dantec 54T33	0.05 to 5 m/s	0–1 m/s: ±2% 1–5 m/s: ±5%

GSD: Geometric standard deviation.

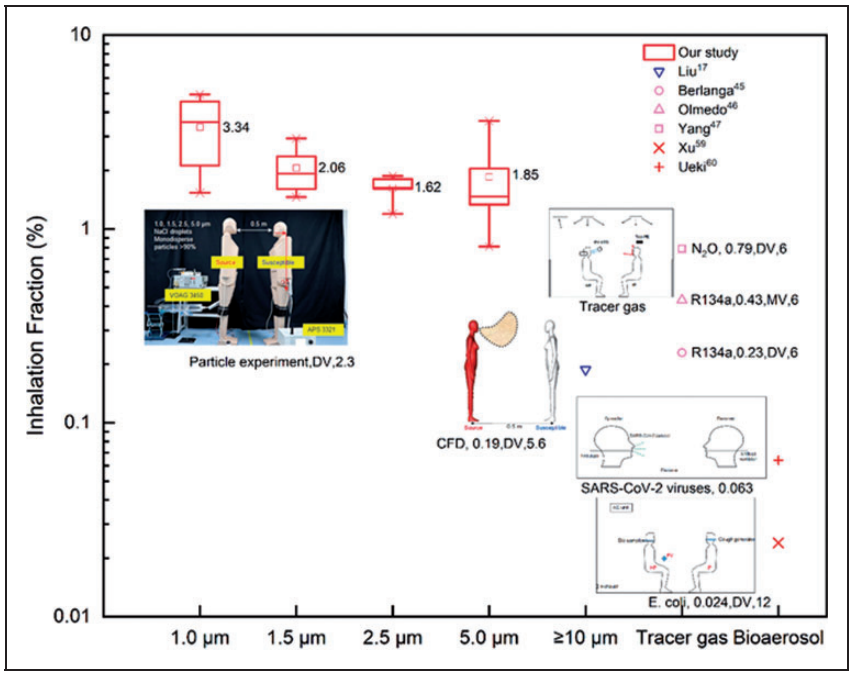

Figure 2. Size-resolved inhalation fraction (IF) for different size distribution over a distance of 0.5 m. Comparison of another study's CFD simulation,[17] tracer gas,[45–47] particle,[57] bioaerosol experiment[59,60]

inhaled particles of the manikin that simulate the susceptible are all the NaCl particles released by our VOAG experiment.

Therefore, the background particle concentration was considered to not influence the experimental data.

The monodispersed particles released by the VOAG 3450 were heated and connected to the manikin's connection port, travelling through a 1.5-m pipe in the manikin's body before being released through the mouth.

Exposure assessment

Our study used index *inhalation fraction* (*IF*), based on the number concentration of droplet nuclei, reflecting the exposure level of the susceptible individual, and considering the characteristics of droplet nuclei size distribution. This is not the same as intake fraction. IF is defined as the ratio of droplet nuclei that can enter the susceptible respiratory tract by inhalation, as given by equation (1)

$$IF = \frac{C_{\text{susceptible}}}{C_{\text{source}}} \tag{1}$$

where C_{source} is the concentration of droplet nuclei released from the source through respiratory activity, and $C_{\text{susceptible}}$ is the concentration inhaled by the susceptible. The *IF* has been previously compared to other exposure assessments and found to provide an accurate estimation of inhalation risk.[17,49,56,57] This index was used by this study.

Results and discussion

We monitored the number of NaCl particles to characterize the transmission and inhalation of virus-laden droplet nuclei in a displacement room. The release, transmission and inhalation of droplet nuclei were similar to NaCl particle. Monodisperse NaCl particles were used to examine the short-range airborne exposure, and the total inhaled particles and *IF* were calculated to explore the infection risk.

In some CFD simulations of the particle diffusion process, users of Lagrangian models commonly claim that statistical reliability has been obtained when the results are independent of increasing the number of particles. Examples include Pascal and Oesterle[58] who compared results using 1×10^4, 2×10^4 and 4×10^4 particles in a simple shear flow and concluded that 2×10^4 were sufficient. The total number of particles released within 1 h for 1.0, 1.5, 2.5, 5.0 μm are 1.27×10^5, 2.46×10^5, 5.47×10^5, 3.0×10^5, respectively, that is far greater than 2×10^4. Hence, the *IF* results are independent of increasing number of particles.

Due to the different source manikin released, we carried out a dimensionless comparison between the source and the susceptible number concentration to

Table 4. Previously reported IFs.

References	*IF* (%)		Distances (m)	Sample\ Simulate time	Source/ type of breath	Posture	Room scale (m)	Ventilation	ACH	Methods
He et al.[48]	Tracer gas	0.0081	>2	–	Mouth	Sitting face-to-back	$4.8 \times 5.4 \times 2.6$	DV	4.3	CFD
	0.8 μm	0.0045								
	5.0 μm	0.0101								
	16 μm	0.0041								
Li et al.[49]	CO_2	0.0085	2	–	Nose	Sitting	$4.0 \times 2.4 \times 3.0$	DV	7.6	CFD
	1.0 μm	0.0085								
	5.0 μm	0.0096								
	10 μm	0.032								
Yang et al. 2015[47]	N_2O	0.79	0.6	30 min	Nose	Sitting	$6.6 \times 4.2 \times 2.7$	DV	6	Experiment
Liu et al.[57]	0.77 μm	4.93	1.1	–	Cough (Latex particle)	Standing	$2.4 \times 2.4 \times 1.5$	DV	3.5	Experiment
	2.5 μm	3.68								
	7.0 μm	1.74								
Liu et al.[17]	100 μm	0.19	0.5	200 s	Breath	Standing	$4.2 \times 3.2 \times 2.7$	DV	5.6	CFD
Berlanga et al.[45]	R134a	0.23	<0.5	360 min	Nose	Standing and prone	$4.5 \times 3.3 \times 2.8$	DV	6	Experiment
Olmedo et al.[46]	R134a	0.43	<0.5	120 min	Nose	Standing and prone	$4.5 \times 3.3 \times 2.8$	MV	6	Experiment
Xu et al.[59]	*Escherichia coli*	0.024	0.5	100 s	Cough	Sitting	$4.0 \times 2.6 \times 2.3$	DV	12	Experiment
		0.011	0.8							
		0.012	1.2							
Ueki et al.[60]	SARS-CoV-2	0.187	0.25	20 min	Cough	Standing	$1.2 \times 0.4 \times 0.5$	–	–	Experiment
		0.063	0.5							
		0.040	1.0							

ACH: Air changes per hour; DV: displacement ventilation; MV: mixing ventilation; Ifs: inhalation fractions; SARS-CoV-2: severe acute respiratory syndrome coronavirus 2.

facilitate the comparison of relative infection risks, that was inhalation fraction (*IF*).

Inhalation fraction for different size distribution

IF in short-range transmission (<0.5 m) has been previously studied using CFD simulation,[17,48,49,57] tracer gases,[45–49] particles[57] and bioaerosol experiments.[59,60] Table 4 lists the results of previous studies wherein the *IF* was calculated using equation (1). Detailed case conditions are also reported in Table 4. Generally, most studies examined breathing and coughing as means for aerosolization of particles.

Two bioaerosol experiments were conducted to indirectly assess the *IF*, as depicted in pink in Figure 2. Xu et al.[59] used *Escherichia coli* to examine the short-range bioaerosol inhalation of cough droplets for different interpersonal distances. The infected individuals were exposed to 0.225×10^6 colony-forming units (CFU) of *E. coli*, while the healthy individuals inhaled 54 CFU (0.5 m), 25 CFU (0.8 m) and 26 CFU (1.2 m). Using equation (1), the corresponding *IFs* can be calculated as 0.024% (0.5 m), 0.011% (0.8 m) and 0.024% (1.2 m). Ueki et al.[60] examined the airborne transmission of SARS-CoV-2 droplets/aerosols between spreaders and receivers who were positioned face-to-face. Ueki's bioaerosol experiment developed an airborne transmission simulator of infectious SARS-CoV-2-containing droplets/aerosols produced by human respiration and coughs, and assessed the transmissibility of the infectious droplets/aerosols. A test chamber for airborne transmission experiments was constructed in a BSL 3 facility, and two mannequin heads were placed facing each other. One mannequin head was connected to a customized compressor nebulizer and exhaled a mist of virus suspension through its mouth to mimic a viral spreader. The other mannequin head was connected to an artificial ventilator through a virus particle collection unit. The airborne transmission simulator is similar to vibrating orifice aerosol generator (VOAG 3450) in this study. The VOAG produces monodisperse NaCl particles to simulate droplet nuclei transmission. Ueki places two mannequin heads face to face and our study employs two standing face-to-face breathing thermal manikins connected to artificial lungs. The initial exhaled particle size was 5.5 ± 0.2 μm. The spreader emitted 5×10^5 plaque forming units (PFU), while the receiver was exposed to 1.072×10^3, 0.316×10^3, and 0.199×10^3 PFU for 0.25 m, 0.5 m, and 1.0 m interpersonal distances, respectively. The *IF*s were therefore calculated as being 0.187%, 0.063% and 0.040%, respectively. Comparing the results of these two

bioaerosol experiments, the calculated *IF*s had the same order of magnitude, although Ueki's *IF*s were larger than that of Xu et al.[59] This may be due to differences in the size of the room, as *IF* and exposure risk have been found to increase with decreasing room size.

Particles between 1.0 and 5.0 μm represent the expiratory aerosols that carry influenza or SARS-CoV-2 viruses. The particle-laden jet is also similar to breathing airflow. In each particle size experiment of our study, the particles were released from the source manikin's mouth at the same gas flow rate. They have the same airflow velocity and the same initial flow state. After entering the indoor environment, the particle-laden jet moved towards the susceptible manikin with the breathing airflow. There was a non-uniform concentration pattern in the test room. The inhaled number of droplet nuclei by susceptible persons was changed instantaneously. During the transmission process, due to different particle sizes, the trajectory of the movement was also changed gradually, and the amount of particles that penetrated the thermal plume of the susceptible manikin to reach the breathing zone was also different, which resulted in a different inhalation fraction. Size is an important factor for the particle transport in the vicinity of the receiver occupant where airflow velocity was decayed to the room background air velocity.

Thus far, we have primarily focused on how the droplet size affected the short-range airborne transmission, during which infection would arise through the inhalation of a critical quantity of airborne pathogens. In our experiments, the source manikin emitted particles while the susceptible manikin was inhaled for a 1-h period. Figure 2 shows the *IF*s calculated for the susceptible manikin based on the concentration of particles exhaled by the source manikin. The *IF*s calculated range from $3.34\% \pm 1.48\%$, $2.06\% \pm 0.60\%$, $1.62\% \pm 0.27\%$ and $1.85\% \pm 1.07\%$ of the total droplets exhaled by the source manikin for particles of 1.0, 1.5, 2.5 and 5.0 μm diameter, respectively, across an interpersonal distance of 0.5 m. The *IF* result of 1.0 μm and 5.0 μm have a long range, and 2.5 μm was concentrated. [AQ1] When ordered by *IF*, $1.0 > 1.5 > 5.0 > 2.5$ μm particles in terms of infective potential. The *IF* of 2.5-μm particles is close to 5.0-μm particles, while the *IF* for 1.0-μm particles is nearly twice that of 2.5-μm and 5.0-μm particles. Large particles are easier to separate with the respiratory flow during the transmission than small particles, and it means that they are less likely to be inhaled by the susceptible manikin. In addition, large particles are more likely to be deposited in the tube inside susceptible manikin, resulting in a reduction of inhaled number. The opposite is true for smaller particles. Hence, the smallest particle resulted in a high inhalation fraction. The distance between source and susceptible individuals was 0.5 m, which falls in the short-range airborne transmission or direct exposure route. These findings conform with the generally accepted rule that the smaller the particle size, the easier it is inhaled and thus the greater the risk of exposure.

When the air change rate was $6\,h^{-1}$ for tracer gas (N_2O, R314a), *IF* results were between 0.23% and 0.79%. Similar results were also obtained with CFD giving 0.19% IF with an air change rate of $5.6\,h^{-1}$. Similar magnitude was found. However, when air change rate of *E. coli* experiment was $12\,h^{-1}$, the result was 0.024% and nearly 3–12.8% of tracer gas experiment and CFD results. The *IF* results of the particle experiment with the displacement ventilation were 1.62–3.34% for $2.3\,h^{-1}$ air change rate and 1.74–4.93% for $3.5\,h^{-1}$ air change rate. Comparing all the results, the conclusion is that under the displacement ventilation strategy, as the number of air changes increased, the *IF* would fall.

Close contact between persons would lead to a higher risk of exposure. An interesting feature to note in Figure 2 is the comparison between CFD simulation and tracer gas results and our own experimental results. Our calculated *IF*s were nearly 10-fold higher than those calculated from CFD simulations, and 2–5-fold higher than those from the tracer gas experiments. CFD techniques have been used to perform high-time-resolution sampling of particle numbers and mass concentrations in the study of many different infectious diseases. However, previous CFD studies were limited to using steady-state Reynolds Average Navier Stokes (RANS) turbulence models to simulate airborne transmissions.[51] CFD simulations generally release a fixed number of particles at one instance during the simulation process, and the simulation time is relatively short (<5 min). In contrast, the actual human breathing is a constant activity that continuously releases particles. As a result, the CFD-simulated *IF*s are often smaller than the corresponding experimental results.

Tracer gases (e.g. CO_2,[49] N_2O,[47] SF_6, and R314a[45,46]) have been widely used to simulate the transmission of exhaled droplet nuclei. However, most tracer gas measurement instruments, including the widely used photoacoustic gas monitors, have a sample time of 10–60 s, which is much longer than the average inspiratory or expiratory duration (~1 s).[51] The sampling time of the tracer gas measuring instrument is not suitable for capturing the detailed evolution of release and inhalation process of droplet nuclei during individual respiratory activities. The inhalation exposure is dynamic, periodic, short and instantaneous. This may lead to inaccurate results, as the low temporal resolution precludes sensitive

detection of rapid changes in particle concentrations. The number distribution of droplet nuclei in the environment after being released is non-uniform, and the inhaled number of droplet nuclei by susceptible persons could also change instantaneously. Therefore, in order to obtain these short-term changes, the sampling interval would need to be smaller and to reflect changes during a respiratory activity. This study generated aerosols and used measurement instruments and breathing thermal manikins to examine the interactions between the respiratory flow and the thermal plume in a cleanroom. By breathing thermal manikin that can produce periodic breathing activities, the sampling interval of the droplet nuclei measurement instrument can be set to 1 s, which can obtain the short and instantaneous change of droplet nuclei inhalation. When the size distribution of droplet nuclei is different, they have various morphologies, shapes, and different physical forces on them, and the virus load laden by droplet nuclei is also different. In order to better simulate this process, compared with the use of tracer gas, the particle experiment may obtain more accurate results.

For particle and bioaerosol experiment, aerosol generation instruments that can more accurately monitor exhaled droplet nuclei transmission have been developed. However, these instruments are generally used alone, rather than in conjunction with breathing thermal manikins. Bioaerosol experiment must be conducted in a high biosafety level facility. To trace SARS-CoV in the laboratory at usual condition is very difficult. If other bacteria are used, the specialty must be considered. The result may not be as good as the particle experiment.

As previously discussed, there are many disadvantages to CFD simulations and tracer gas experiments, limiting the generalizability of their results. This study generated aerosols and used measurement instruments and breathing thermal manikins to examine the interactions between respiratory flow and thermal plume in a cleanroom. Therefore, the results of our experiments are likely highly reflective of physiological conditions.

Inhalation fraction for different interpersonal distances

The number of droplets inhaled and thus *IF* were inversely proportional to the distance between the source manikin and the susceptible manikin. As a result, for close-range interactions, exposure risk would be reduced as the interpersonal distance is increased. When the expiratory jet spread angle is narrowed, passive tracer gas decay would follow the $1/d$ rule, where d is the interpersonal distance. However, when the jet spread angle is wide, the $1/d^2$ rule would be applied.[61]

Figure 3 depicts the *IF* results from the studies described in Table 4. We listed four different methods

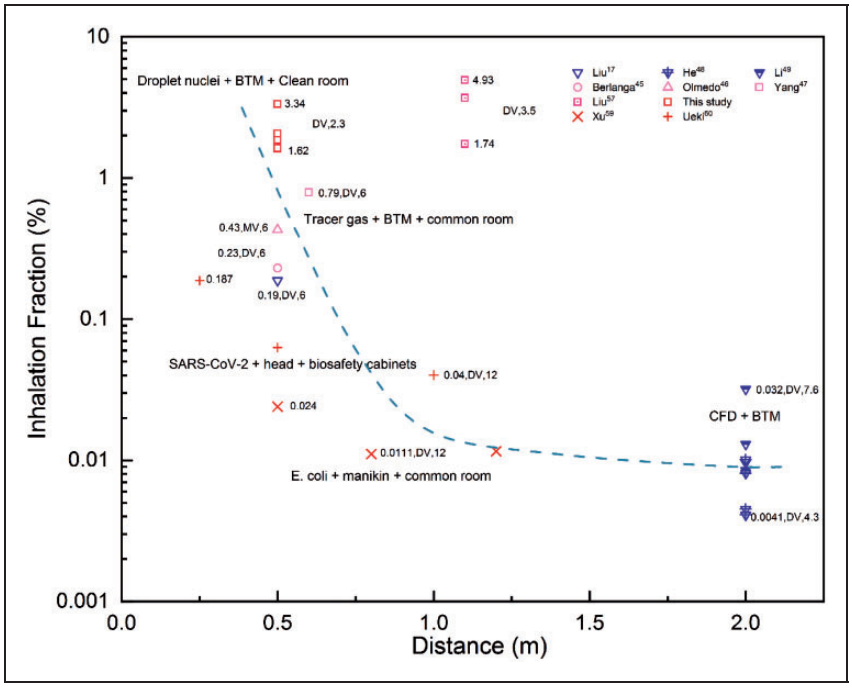

Figure 3. Inhalation fraction for different interpersonal distances. The boundary conditions (ventilation strategies and air change rate) and IF results of CFD simulation, tracer gas, particle and bioaerosol experiment were enumerated during short-range airborne transmission. The *IF* was reduced as the interpersonal distance was increased, as shown by the blue dotted line and IFs decay follows 1/d rule.

for *IF* researches: the CFD simulation with a computer manikin in a full-scale room,[48,49] the tracer gas experiment with a manikin in a full-scale room,[45–47] the particle experiment with a manikin in a cleanroom (our study) and the bioaerosol experiment in a biosafety facility.[59,60] He et al.[48] and Li et al.[49] used CFD simulations to evaluate *IF*s at a distance of 2 m, and their results were broadly in agreement. The *IF*s calculated for a distance of 2 m were lower than those in studies conducted at distances of 0.5 m or 1.0 m. Berlnaga et al.,[45] Olmedo et al.[46] and Yang et al.[47] used tracer gases and calculated *IF*s falling within the same order of magnitude. Xu et al.[59] and Ueki et al.[60] used bioaerosols, and the corresponding *IF*s was shown to have declined. *IF* results may vary within the mean range of 0.011–0.187%.

In the case of the present study, our experimentally calculated *IF*s and those of Liu et al.[57] were particle experiments. Moreover, both sets of *IF*s have the same order of magnitude. Liu et al.[57] used latex spherical monodispersed particles to examine the impact of particle size on particle transport in close proximity to cough events. Similar to this study, Liu et al. used thermal manikins, but their manikins were rectangular parallelepiped in shape and thus did not reflected the true shape of the human body. Due to the strength of a coughing event, even though the interpersonal distance was greater than that was used in the present study, their calculated *IF*s (0.77 μm and 2.5 μm) exceeded those calculated in this study for normal breathing. However, we observed a similar trend whereby the *IF* was decreased with the increase of particle sizes.

The results in Table 4 and Figure 3 showed that the particle-based experimental results resulted in larger *IF* values than the other three types of experiments. Moreover, the CFD results resembled the bioaerosol results, in that, they both resulted in lower *IF* values than other experiments. This may be because bioaerosol sampling would require post-cultivation.

Finally, we fitted a curve to the plot of *IF* versus interpersonal distance, incorporating all data points. This curve aligned well with the $1/d$ rule, thus confirming the practicability of the 'Six-Foot Rule' in mitigating indoor airborne transmission in the time of COVID-19.

Limitation and future research

The study used breathing thermal manikins to evaluate the number of inhaled particles and the corresponding *IF* in a displacement ventilated indoor environment. Due to the triple planar and non-planar bifurcations of the human respiratory system, models of the system are complicated.[62] The sampling tube in our experiment runs from the nose through the thermal manikin's body (see Figure 1), and we did not consider the airflow structures present in the branching lung airway. The human respiratory system is saturated with humidity and body fluids, which could greatly influence the droplet formation and respiration, and we have not considered these in our model. Thus, we require delicate design of the mouth and the lung structure to make the human respiratory tract mode more realistic. Our research can thus be further improved upon by using breathing thermal manikins with 3 D printed respiratory tracts filled with saturated, humidified air to mimic the physiological conditions.

Additionally, droplets smaller than 50 μm were suspended and were mostly carried within respiratory flow. Thus, such droplets could deviate from the expired jet and could settle 1–2 m away, or can be deposited on the face.[61] Future studies should examine the transmission of airborne particles ≤ 50 μm and their deposition on the body's surface, including the face, mouth and eye mucous membrane.

Conclusions

In this study, we used breathing thermal manikins to estimate interpersonal viral exposure using inhaled particle numbers and *IF*s in a full-scale ventilated room. The study focused on the effect of the droplet nuclei size distribution on the short-range airborne transmission. The results indicated that the particle size distribution exhibits different dynamics in the vicinity of a susceptible individual. The droplet nuclei diameter was shown to have an important effect on transmission. The *IF* was found to decrease with the increasing of particle size. Additionally, we compared the effect of distances on transmission, incorporating the findings of other studies, and concluded that the *IF* would decrease with an increasing of the interpersonal distance, fitting well with the $1/d$ rule.

This study highlights the value of the *IF* index, which can be used to characterize the exposure risk in experiments using CFD simulations, tracer gas, particles and bioaerosols. Our data will provide a quantitative basis to inform infection control policy and provide insight into the transmission mechanisms of SARS-CoV-2.

Authors contribution

All authors contributed equally in the preparation of this manuscript.

Acknowledgements

We acknowledge State Key Laboratory of Green Building in Western China for the use of full-scale cleanroom and Aalborg University for the supply of two breathing thermal manikin and artificial ventilator. Special thanks to Wang Lijuan and Meng Xingyan for their work in the experiment.

Declaration of conflicting interests

The author(s) declared no potential conflicts of interest with respect to the research, authorship, and/or publication of this article.

Funding

The author(s) disclosed receipt of the following financial support for the research, authorship, and/or publication of this article: This research was financially sponsored by the National Key Research and Development Program of China (grant no. 2020YFC0861500), the National Natural Science Foundation of China (grant no. 51778520) and Education Department Key Project of Shaanxi Province (grant no. 20JS077).

ORCID iDs

Linzhi Fu https://orcid.org/0000-0001-7492-6832
Li Liu https://orcid.org/0000-0001-8512-8676

References

1. Tang JW, Bahnfleth WP, Bluyssen PM, Buonanno G, Jimenez JL, Kurnitski J, Li Y, Miller S, Sekhar C, Morawska L, Marr LC, Melikov AK, Nazaroff WW, Nielsen PV, Tellier R, Wargocki P and Dancer SJ. Dismantling myths on the airborne transmission of severe acute respiratory syndrome coronavirus-2 (SARS-CoV-2). *J Hospital Infect* 2021; 110: 89–96.
2. Shiu EY, Leung NH and Cowling BJ. Controversy around airborne versus droplet transmission of respiratory viruses: implication for infection prevention. *Curr Opin Infect Dis* 2019; 32: 372–379.
3. Greenhalgh T, Jimenez JL, Prather KA, Tufekci Z, Fisman D and Schooley R. Ten scientific reasons in support of airborne transmission of SARS-CoV-2. *Lancet* 2021; 397: 1603–1605.
4. Morawska L and Cao J. Airborne transmission of SARS-CoV-2: the world should face the reality. *Environ Int* 2020; 139: 105730.
5. Allen JG and Ibrahim AM. Indoor air changes and potential implications for SARS-CoV-2 transmission. *JAMA* 2021; 325: 2112–2113.
6. Xu C, Luo X, Yu C and Cao S-J. The 2019-nCoV epidemic control strategies and future challenges of building healthy smart cities. *Indoor Built Environ* 2020; 29: 639–644.
7. CDC. How COVID-19 Spreads, https://www.cdc.gov/coronavirus/2019-ncov/prevent-getting-sick/how-covid-spreads.html (accessed 13 May 2021).
8. Organization WH. *Transmission of SARS-CoV-2: implications for infection prevention precautions: scientific brief, 09 July 2020*. Geneva: World Health Organization, 2020.
9. Qian H, Miao T, Liu L, Zheng X, Luo D and Li Y. Indoor transmission of SARS-CoV-2. *Indoor Air* 2021; 31: 639–645.
10. Sun K, Wang W, Gao L, Wang Y, Luo K, Ren L, Zhan Z, Chen X, Zhao S and Huang Y. Transmission heterogeneities, kinetics, and controllability of SARS-CoV-2. *Science* 2021; 371: eabe2424.
11. Allen JG and Marr LC. Recognizing and controlling airborne transmission of SARS-CoV-2 in indoor environments. *Indoor Air* 2020; 30: 557–558.
12. Zhang N, Tang JW and Li Y. Human behavior during close contact in a graduate student office. *Indoor Air* 2019; 29: 577–590.
13. Prather KA, Marr LC, Schooley RT, McDiarmid MA, Wilson ME, and Milton DK. Airborne transmission of SARS-CoV-2. *Science* 2020; 370: 303–304.
14. Li YG. Basic routes of transmission of respiratory pathogens – a new proposal for transmission categorization based on respiratory spray, inhalation, and touch. *Indoor Air* 2021; 31: 3–6.
15. Chen W, Zhang N, Wei J, Yen H-L and Li Y. Short-range airborne route dominates exposure of respiratory infection during close contact. *Build Environ* 2020; 176: 106859.
16. Morawska L and Milton DK. It is time to address airborne transmission of coronavirus disease 2019 (COVID-19). *Clin Infect Dis* 2020; 71: 2311–2313.
17. Liu L, Li Y, Nielsen PV, Wei J and Jensen RL. Short-range airborne transmission of expiratory droplets between two people. *Indoor Air* 2017; 27: 452–462.
18. Morawska L and Buonanno G. The physics of particle formation and deposition during breathing. *Nat Rev Phys* 2021; 3: 300–301.
19. Klompas M, Baker MA and Rhee C. Airborne transmission of SARS-CoV-2: theoretical considerations and available evidence. *JAMA* 2020; 324: 441–442.
20. Samet JM, Prather K, Benjamin G, Lakdawala S, Lowe J-M, Reingold A, Volckens J and Marr LC. Airborne transmission of severe acute respiratory syndrome coronavirus 2 (SARS-CoV-2): what we know. *Clin Infect Dis* 2021; ciab039, https://doi.org/10.1093/cid/ciab039 [AQ2]
21. Drossinos Y and Stilianakis NI. What aerosol physics tells us about airborne pathogen transmission. *Aerosol Sci Technol* 2020; 54: 639–643.
22. Ding J, Yu CW and Cao S-J. HVAC systems for environmental control to minimize the COVID-19 infection. *Indoor Built Environ* 2020; 29: 1195–1201.
23. Fennelly KP. Particle sizes of infectious aerosols: implications for infection control. *Lancet Respir Med* 2020; 8: 914–924.
24. Yan J, Grantham M, Pantelic J, de Mesquita PJB, Albert B, Liu F, Ehrman S, Milton DK and Consortium E. Infectious virus in exhaled breath of symptomatic seasonal influenza cases from a college community. *Proc Natl Acad Sci U S A* 2018; 115: 1081–1086.
25. Bake B, Larsson P, Ljungkvist G, Ljungström E and Olin A. Exhaled particles and small airways. *Respir Res* 2019; 20: 14.
26. Liu Y, Ning Z, Chen Y, Guo M, Liu Y, Gali NK, Sun L, Duan Y, Cai J and Westerdahl D. Aerodynamic analysis of SARS-CoV-2 in two Wuhan hospitals. *Nature* 2020; 582: 557–560.
27. Chia PY, Coleman KK, Tan YK, Ong SWX, Gum M, Lau SK, Lim XF, Lim AS, Sutjipto S and Lee PH. Detection of air and surface contamination by SARS-CoV-2 in hospital rooms of infected patients. *Nat Commun* 2020; 11: 1–7.

28. Van Doremalen N, Bushmaker T, Morris DH, Holbrook MG, Gamble A, Williamson BN, Tamin A, Harcourt JL, Thornburg NJ and Gerber SI. Aerosol and surface stability of SARS-CoV-2 as compared with SARS-CoV-1. *N Engl J Med* 2020; 382: 1564–1567.
29. Alsved M, Matamis A, Bohlin R, Richter M, Bengtsson P-E, Fraenkel C-J, Medstrand P and Löndahl J. Exhaled respiratory particles during singing and talking. *Aerosol Sci Technol* 2020; 54: 1245–1248.
30. Lee BU. Minimum sizes of respiratory particles carrying sars-cov-2 and the possibility of aerosol generation. *Int J Environ Res Public Health* 2020; 17: 6960.
31. Duguid J. The numbers and the sites of origin of the droplets expelled during expiratory activities. *Edinb Med J* 1945; 52: 385.
32. Loudon RG and Roberts RM. Droplet expulsion from the respiratory tract. *Am Rev Respir Dis* 1967; 95: 435–442.
33. Papineni RS and Rosenthal FS. The size distribution of droplets in the exhaled breath of healthy human subjects. *J Aerosol Med* 1997; 10: 105–116.
34. Chao CYH, Wan MP, Morawska L, Johnson GR, Ristovski Z, Hargreaves M, Mengersen K, Corbett S, Li Y and Xie X. Characterization of expiration air jets and droplet size distributions immediately at the mouth opening. *J Aerosol Sci* 2009; 40: 122–133.
35. Morawska L, Johnson G, Ristovski Z, Hargreaves M, Mengersen K, Corbett S, Chao CYH, Li Y and Katoshevski D. Size distribution and sites of origin of droplets expelled from the human respiratory tract during expiratory activities. *J Aerosol Sci* 2009; 40: 256–269.
36. Asadi S, Wexler AS, Cappa CD, Barreda S, Bouvier NM and Ristenpart WD. Aerosol emission and superemission during human speech increase with voice loudness. *Sci Rep* 2019; 9: 1–10.
37. Asadi S, Bouvier N, Wexler AS and Ristenpart WD. The coronavirus pandemic and aerosols: does COVID-19 transmit via expiratory particles? *Aerosol Sci Technol* 2020; 54: 635–638.
38. Hartmann A, Lange J, Rotheudt H and Kriegel M. Emission rate and particle size of bioaerosols during breathing, speaking and coughing. *DepositOnce* 2020; 226493262. DOI: 10.14279/depositonce-10331. **[AQ3]**
39. Li L, Niu M and Zhu Y. Assessing the effectiveness of using various face coverings to mitigate the transport of airborne particles produced by coughing indoors. *Aerosol Sci Technol* 2021; 55: 332–339.
40. Mürbe D, Kriegel M, Lange J, Schumann L, Hartmann A and Fleischer M. Aerosol emission of adolescents voices during speaking, singing and shouting. *PLoS One* 2021; 16: e0246819.
41. Hamilton F, Gregson F, Arnold D, Sheikh S, Ward K, Brown J, Moran E, White C, Morley A, Bzdek B, Reid J, Maskell N and Dodd JW. Aerosol emission from the respiratory tract: an analysis of relative risks from oxygen delivery systems. *medRxiv Preprint 2021*. DOI: 10.1101/2021.01.29.21250552. **[AQ4]**
42. Gregson FKA, Watson NA, Orton CM, Haddrell AE, McCarthy LP, Finnie TJR, Gent N, Donaldson GC, Shah PL, Calder JD, Bzdek BR, Costello D and Reid JP. Comparing aerosol concentrations and particle size distributions generated by singing, speaking and breathing. *Aerosol Sci Technol* 2021; 55: 681–691.
43. Sayampanathan AA, Heng CS, Pin PH, Pang J, Leong TY and Lee VJ. Infectivity of asymptomatic versus symptomatic COVID-19. *Lancet* 2021; 397: 93–94.
44. Lindsley WG, Blachere FM, Beezhold DH, Thewlis RE, Noorbakhsh B, Othumpangat S, Goldsmith WT, McMillen CM, Andrew ME and Burrell CN. Viable influenza A virus in airborne particles expelled during coughs versus exhalations. *Influenza Other Respir Viruses* 2016; 10: 404–413.
45. Berlanga F, de Adana MR, Olmedo I, Villafruela J, San José J and Castro F. Experimental evaluation of thermal comfort, ventilation performance indices and exposure to airborne contaminant in an airborne infection isolation room equipped with a displacement air distribution system. *Energ Build* 2018; 158: 209–221.
46. Olmedo I, Berlanga F, Villafruela J and De Adana MR. Experimental variation of the personal exposure in a hospital room influenced by wall heat gains. *Build Environ* 2019; 154: 252–262.
47. Yang J, Sekhar S, Cheong K and Raphael B. Performance evaluation of a novel personalized ventilation–personalized exhaust system for airborne infection control. *Indoor Air* 2015; 25: 176–187.
48. He Q, Niu J, Gao N, Zhu T and Wu J. CFD study of exhaled droplet transmission between occupants under different ventilation strategies in a typical office room. *Build Environ* 2011; 46: 397–408.
49. Li X, Niu J and Gao N. Co-occupant's exposure to exhaled pollutants with two types of personalized ventilation strategies under mixing and displacement ventilation systems. *Indoor Air* 2013; 23: 162–171.
50. Xu C and Liu L. Personalized ventilation: One possible solution for airborne infection control in highly occupied space? *Indoor Built Environ* 2018; 27: 873–876.
51. Ai Z, Hashimoto K and Melikov AK. Airborne transmission between room occupants during short-term events: measurement and evaluation. *Indoor Air* 2019; 29: 563–576.
52. Nielsen PV, Buus M, Winther FV and Thilageswaran M. Contaminant flow in the microenvironment between people under different ventilation conditions. *ASHRAE Trans* 2008; 114: 632–638.
53. Olmedo I, Nielsen PV, Ruiz de Adana M and Jensen RL. The risk of airborne cross-infection in a room with vertical low-velocity ventilation. *Indoor Air* 2013; 23: 62–73.
54. Olmedo I, Nielsen PV, Ruiz de Adana M, Jensen RL and Grzelecki P. Distribution of exhaled contaminants and personal exposure in a room using three different air distribution strategies. *Indoor Air* 2012; 22: 64–76.
55. Bjørn E and Nielsen PV. Dispersal of exhaled air and personal exposure in displacement ventilated rooms. *Indoor Air* 2002; 12: 147–164.

56. Li X, Niu J and Gao N. Spatial distribution of human respiratory droplet residuals and exposure risk for the co-occupant under different ventilation methods. *HVAC&R Res* 2011; 17: 432–445.
57. Liu S and Novoselac A. Transport of airborne particles from an unobstructed cough jet. *Aerosol Sci Tech* 2014; 48: 1183–1194.
58. Pascal P and Oesterlé B. On the dispersion of discrete particles moving in a turbulent shear flow. *Int J Multiphase Flow* 2000; 26: 293–325.
59. Xu JC, Wang CT, Fu SC, Chan KC and Chao CYH. Short-range bioaerosol deposition and inhalation of cough droplets and performance of personalized ventilation. *Aerosol Sci Tech* 2021; 55: 474–485.
60. Ueki H, Furusawa Y, Iwatsuki-Horimoto K, Imai M, Kabata H, Nishimura H, Kawaoka Y and Imperiale MJ. Effectiveness of face masks in preventing airborne transmission of SARS-CoV-2. *mSphere* 2020; 5: 00620 e00637.
61. Li YG. The respiratory infection inhalation route continuum. *Indoor Air* 2021; 31: 279–281.
62. Zhang Z and Kleinstreuer C. Transient airflow structures and particle transport in a sequentially branching lung airway model. *Phys Fluid* 2002; 14: 862–880.